



Cite this: *Dalton Trans.*, 2019, **48**, 9920

Received 1st June 2019,
Accepted 5th June 2019

DOI: 10.1039/c9dt02313e

rsc.li/dalton

Direct oxide transfer from an η^2 -keto ligand to generate a cobalt PC_{carbene}P(O) pincer complex†

Simon Sung,^a Hendrik Tinnermann,^a Tobias Krämer^{b*} and Rowan D. Young^{a*}

We report the direct carbonyl cleavage in a κ^3 -P',(η^2 -C,O),P'' ligand by a monomeric cobalt centre through metal–ligand cooperativity. C–O cleavage leads to the formation of a PC_{carbene}P(O) pincer ligand with a central alkylidene anchor. A DFT analysis, supported by kinetic studies, suggests that decoordination of a pincer phosphino arm to generate a kinetically accessible free phosphine may be critical in transfer of the oxide to a phosphorus position. Thus, oxide transfer to bisphosphino bidentate co-ligands was also found to be viable, allowing access to the previously reported PC_{carbene}P pincer complex (2), where bisphosphines were used as oxide sequestering agents.

The direct cleavage of carbon–oxygen multiple bonds is an important step in carbon–carbon bond forming processes, such as the Fischer–Tropsch synthesis (FTS) and the McMurry reaction. In such reactions, it is proposed that direct C–O bond cleavage of CO or ketones gives rise to metal–carbenoid intermediates.¹ Despite the importance of such reactions, the observation of carbon–oxygen multiple bond cleavage is exceedingly rare in homogenous chemistry, limiting our understanding of these processes. Indeed, observations of the formation of metal alkylidenes *via* direct C–O bond cleavage is limited to a handful of reports. Meyer reported the oxidative addition of cyclopentanone to tungsten, generating terminal oxo and alkylidene ligands (Fig. 1(A)),² Gade demonstrated the addition of cyclopropanone to a bimetallic Fe–Zr complex (Fig. 1(B)),³ and Thomas employed a bimetallic Co–Zr complex to cleave the C–O bond in benzophenone, generating a cobalt alkylidene with a bridging oxide ligand (Fig. 1(C)).⁴ In related chemistry, Braunschweig has also demonstrated the meta-thesis of ketones with metal borylene complexes to generate alkylidene complexes on manganese.⁵

Although late transition metals are competent catalysts in FTS, as well as other oxide transfer reactions, the process of oxide transfer in such systems is not well understood, with terminal and bridging oxo intermediates possible in this process. However, isolated examples of late transition metal terminal oxo complexes are rare. Indeed, the extent of isolated low-valent late transition metal oxo complexes is limited to a Re(I) oxo complex featuring a strongly electron withdrawing ligand (not structurally characterized), a square planar platinum oxo complex (not structurally characterized) and a terminal cobalt(III) oxide in a tetrahedral ligand field.^{6–8} In contrast, metal clusters are reported to cleave carbon–oxygen bonds in carbon monoxide and ketones generating bridging oxides,⁹ implying that oxide transfer in such processes may not be a monometallic process, and may proceed *via* bridging oxides.

Carbon–oxygen bond cleavage by multimetallic systems is unsurprising given the enhanced reactivity of bimetallic cooperation is well documented in many chemical systems.¹⁰ More recently, metal–ligand cooperativity in pincer ligands (rigid tridentate, meridional ligands) has been exploited to enact difficult bond cleavage by monometallic systems (*e.g.*

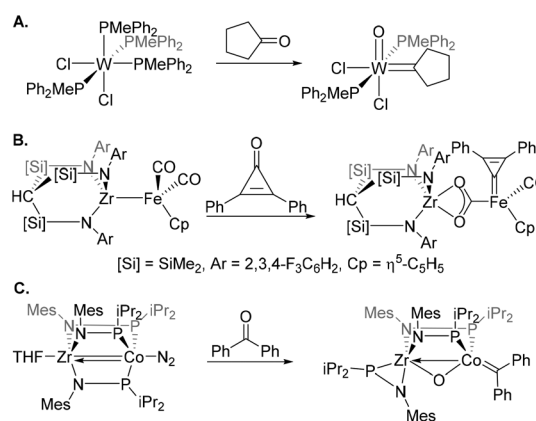


Fig. 1 Previously examples of carbonyl cleavage resulting in alkylidene complexes. A. Ref. 2, B. ref. 3, C. ref. 4.

^aDepartment of Chemistry, National University of Singapore, 3 Science Drive 3, Singapore 117543, Singapore. E-mail: rowan.young@nus.edu.sg

^bDepartment of Chemistry, Maynooth University, Maynooth, Co. Kildare, Ireland

† Electronic supplementary information (ESI) available. CCDC 1882099 and 1908199–1908201. For ESI and crystallographic data in CIF or other electronic format see DOI: 10.1039/c9dt02313e

H–H, C–H, N–H, O–H activations).¹¹ In such systems, rather than simply supporting the metal centre, the pincer ligand actively partakes in reactivity, lowering the relative kinetic barrier to bond cleavage.

Indeed, oxide transfer in pincer complexes featuring phosphino donors often results in sequestration of the oxide unit by a phosphino constituent within in the pincer ligand framework.^{6,12} Piers and Maron recently demonstrated that such transfers did not necessitate transient terminal oxo species, and direct oxide insertion (from an amine oxide source) into metal phosphorus bonds of a PCP pincer ligand is possible.^{12a} To understand both C–O bond cleavage and oxide transfer we have focused on metals ligated by a POP bisphosphinoketone ligand (A, Fig. 2) that can bind in a $\kappa^3\text{-P}(\eta^2\text{-C,O})$, P' fashion. Herein, we report metal–ligand cooperativity in a rare direct cleavage of a keto carbon–oxygen double bond.

Recently, we reported the reduction of ligand A present on cobalt complex 1 to the corresponding $\text{PC}_{\text{carbene}}\text{P}$ alkylidene pincer complex 2 (Fig. 2).¹³ This process was reliant on an equivalent of hydrogen gas as a reducing agent. However, heating samples of 1 in toluene above 100 °C leads to the formation of compound 3 over the period of 12 hours in 91% isolated yield. Astonishingly, 3 represents direct access to an alkylidene pincer ligand, for which there has been much interest in recent literature due to the ability of such ligands to partake in ligand cooperativity through the metal–alkylidene linkage.^{13,14}

The migration of the oxide group to a pincer flanking phosphino group is evident in the ³¹P NMR spectrum that displays a sharp signal at δ_{P} 48.7 ppm devoid of coupling to other phosphorus atoms in the cobalt coordination sphere. The three remaining phosphino ligand signals for 3 appear broadened in the ³¹P NMR spectrum, but at 253 K are resolved into two sets of signals representing two isomeric forms of 3. Based on the ratio of the two isomers (2 : 1), the free energy difference (ΔG) at 253 K is *ca* -0.4 kcal mol⁻¹. Computationally derived structures of 3 estimate a free energy difference of -1.7 kcal mol⁻¹ at 298 K between the isomeric forms, in close agreement with the experimental value (ESI, Fig. S39†). The

¹³C NMR spectrum of 3 reveals a broad signal at 176.3 ppm that is shown to correlate to aromatic protons in the pincer backbone in a HMBC spectrum, and is assigned as the carbeneic ¹³C signal.

An X-ray crystal structure of one of the diastereomers of 3 (Fig. 3, top) supported the formation of an alkylidene ligand, and confirmed the migration of the oxide to a *cis* phosphino position. The observed Co1–C1 bond distance in 3 of 1.930(4) Å is within reported distances for cobalt carbene linkages, but slightly longer than that observed for the carbene linkage in 2 of 1.892(3) Å.¹³ This elongation may arise from a geometric distortion upon the formation of a six-membered metallacyclic ring in 3, as opposed to the preferred five-membered metallacyclic rings present in 2. Alternatively, reduced retrodonation and π -bond character in the Co=C bond arising from a lower Co electron density resultant from replacement of a phosphine donor with an oxide donor may contribute to the bond elongation.^{12a}

The molecular structure of 3 reveals a large torsion angle of 48.7(3)° between the two phenylene rings that constitute the pincer's backbone. This angle is much greater than the

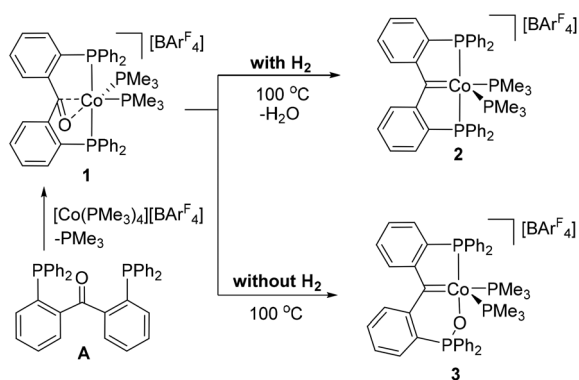


Fig. 2 Reaction of 1 at 100 °C in the presence (top)¹³ and absence (bottom) of hydrogen.

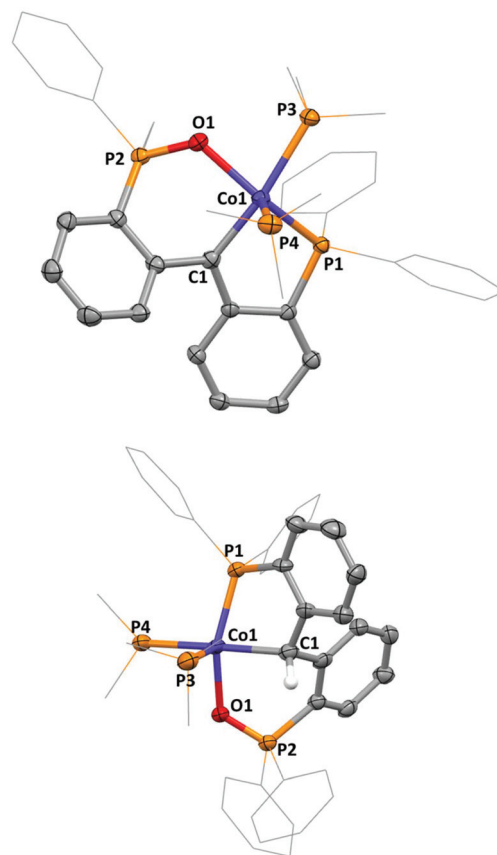


Fig. 3 Molecular structures of 3 (top) and 4 (bottom). Hydrogen atoms and anions omitted, thermal ellipsoids shown at 50%. Selected bond distances (Å) and angles (°), 3: Co1–P1, 2.176(1); Co1–C1, 1.930(4); Co1–O1, 2.010(3); Co1–P3, 2.266(1); Co1–P4, 2.228(1); C1–Co1–P3 165.4(1); P1–Co1–O1, 147.6(1), 4: Co1–P1, 2.169(2); Co1–C1, 2.080(7); Co1–O1, 2.029(4); P1–Co1–O1 150.0(1).

observed torsion angle of $39.8(2)^\circ$ between the pincer's phenylene motifs in **2**, and may account for the barrier of interconversion for the isomers of **3**, which is not observed in **2** at low temperatures.

Attempts to deoxygenate **3** via transfer of the oxo group to added excess PMe_3 to generate **2** failed to result in any reaction, even upon heating to 130°C for 17 hours (Fig. 4). The addition of hydrogen to **3** at room temperature also failed to provide any evidence for the formation of **2**, with neither **2** nor its liberated hydrogenated pincer ligand $\{\text{CH}_2(2\text{-PPh}_2\text{-C}_6\text{H}_4)_2\}$ observed via ^{31}P NMR spectroscopy or mass spectrometry. Rather hydrogenation of **3** resulted in a one electron oxidation of the cobalt centre and generation of the $\kappa^3\text{-PC(H)P(O)}$ complex **4** (Fig. 3, bottom), where the alkylidene centre of **3** was transformed into an sp^3 centre (Fig. 4). Although complex **4** was only isolated via crystallization in 62% yield, it is NMR silent (rendering *in situ* yield difficult to obtain), and no other cobalt containing products were identified via mass spectrometry. As compound **1** has been shown to generate **2** in the presence of hydrogen, it would appear that the oxide transfer from **1** to **3** is an irreversible process.

Monitoring samples of **1** at temperatures above 100°C showed the conversion to **3** to be quantitative based on ^{31}P NMR. As such, kinetic data for the transformation of **1** to **3** were obtained from 90°C to 120°C in xylenes solvent. From these data, an activation energy of $24.8 \pm 2.0 \text{ kcal mol}^{-1}$ was derived from an Arrhenius Plot (ESI, Fig. S2†).

In order to gain insight into the mechanism underlying the formation of **3** and the chemical process that represents the above barrier, the oxide transfer reaction was further studied by density functional theory (DFT) calculations at the SMD-B97D3/6-31++G(2d,p)//BP86/SDD/6-31G(d,p) level of theory.

Optimized geometries of all species discussed in this section are found in the ESI.† A plausible low-energy reaction pathway connecting **1** to **3** is shown in Fig. 5. The initial step of the reaction involves decooordination of one of the phosphine arms of the pincer ligand via $\text{TS}_{\text{decoord}}$ ($\Delta G^\ddagger = 12.4 \text{ kcal mol}^{-1}$), generating intermediate **1'** ($10.4 \text{ kcal mol}^{-1}$) with a free but closely located phosphine ($\text{Co}\cdots\text{P2}$ calc. 3.96 \AA). In the second step oxygen transfer from the carbonyl group to phosphorus occurs via $\text{TS}_{\text{P-O}}$ and an associated barrier of $\Delta G^\ddagger = 26.8 \text{ kcal mol}^{-1}$. The optimized geometry of this transition

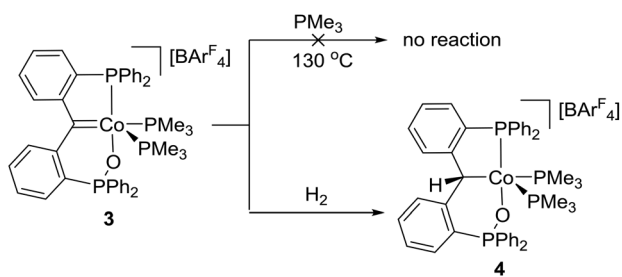


Fig. 4 Attempts to deoxygenate **3** with sacrificial PMe_3 (top) and hydrogen gas (bottom), which instead generates **4**.

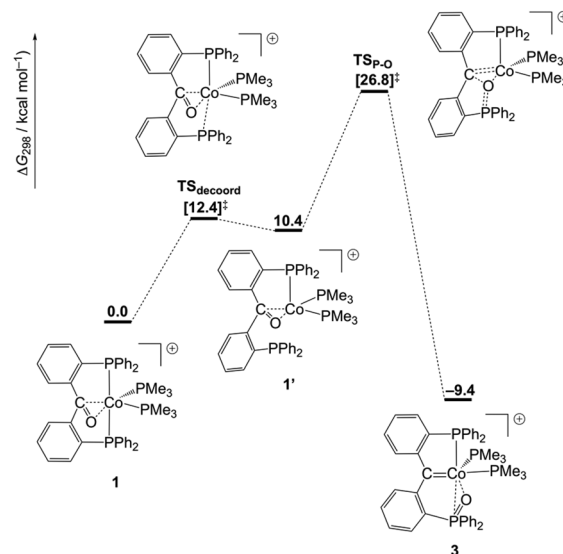


Fig. 5 Calculated free energy surface (SMD-B97D3/6-31++G(2d,p)//BP86/SDD/6-31G(d,p)) for the oxide transfer to generate **3** from **1**.

state displays considerable lengthening of the $\text{C}=\text{O}$ bond distance ($\text{C}=\text{O}$ calc. 1.49 \AA) relative to the reactant complex **1** (calc. 1.35 \AA). Concomitantly, the $\text{Co}-\text{C}$ and $\text{P}-\text{O}$ distances shorten to 1.98 \AA and 1.88 \AA , respectively, indicating a significant degree of carbon-cobalt and oxygen-phosphorus bonding in the transition state. Oxidation of the phosphine is exergonic by $9.4 \text{ kcal mol}^{-1}$, rendering this reaction irreversible, as suggested above. In the optimized geometry of the product complex **3** the $\text{Co}-\text{C}$ and $\text{Co}-\text{O}$ bond distances are 1.90 \AA (exp. $1.930(4) \text{ \AA}$) and 2.05 \AA (exp. $2.010(3) \text{ \AA}$), respectively, in very good agreement with their experimental counterparts. The bond distances of the basal $\text{Co}-\text{P}$ bonds *trans* to phosphine ($\text{Co}-\text{P1}$ calc. 2.21 \AA , exp. $2.176(1) \text{ \AA}$) and alkylidene ($\text{Co}-\text{P3}$ calc. 2.31 \AA , exp. $2.266(1) \text{ \AA}$) reflect the same asymmetry as seen in the X-ray crystal structure. The phosphorus-oxygen bond distance ($\text{P}-\text{O}$ calc. 1.58 \AA) is slightly elongated relative to the free ligand (calc. 1.54 \AA). In an alternative pathway, direct insertion of the oxygen atom into the $\text{Co}-\text{P}$ bond can also occur through a transition state $\text{TS}'_{\text{P-O}}$ that is only slightly higher in energy than $\text{TS}_{\text{P-O}}$ ($\Delta G^\ddagger = 27.5 \text{ kcal mol}^{-1}$, ESI, Fig. S36†). The calculated overall free energy barriers for both the above processes are in good agreement with the experimentally determined value, although it appears that this originates from favorable error cancellation of enthalpic and entropic energy terms. Whilst the second pathway seems less compatible with the negative ΔS^\ddagger , the present molecular model cannot discriminate between the one- and two-step pathways based on their entropies of activation. The accurate estimation of solution phase entropies remains a considerable challenge for computational chemistry owing to the fact that most molecular models are based on the ideal gas approximation.¹⁵ In both cases the calculations predict slightly positive values for ΔS^\ddagger , which may be attributed to the neglect of weak intermolecular interactions and bulk solvation effects in the

present computational model. Nonetheless, both such direct insertion mechanisms closely mirror the proposed mechanism for oxide insertion into nickel–phosphorus bonds delivered by amine oxide reagents suggested by Piers and Maron.^{12a} A more rigorous approach utilizing extensive configurational sampling techniques to obtain highly accurate activation parameters¹⁶ is beyond the scope of this contribution. Another possible pathway involving a terminal cobalt oxo species was also probed. Geometry minimization of such a putative cobalt oxo intermediate in its electronic triplet ($S = 1$) ground state afforded a complex that is prohibitively high in energy (>50 kcal mol⁻¹) to allow for any participation in the above oxide transfer. Furthermore, from analysis of its spin density distribution the electronic structure of this species is best described as Co oxyl complex with significant PCP ligand radical character (ESI, Fig. S37†). Loss of one ancillary PMe₃ ligand does not help to significantly stabilize the Co oxyl species, and the resulting complex lies equally high in energy following geometry optimization (~ 42 kcal mol⁻¹). As such, the involvement of such terminal cobalt oxo intermediates along the reaction pathway is highly improbable.

The realization that kinetic factors may control oxide transfer to an adjacent pendant phosphorus atom (see **1'**, Fig. 5) may explain the lack of oxide transfer to PMe₃, and persuaded us to focus on chelate bisphosphino co-ligands for the generation of **2** from **1** using other phosphines as oxide acceptors. We reasoned that chelate bisphosphino ligands may be more susceptible to partial decoordination as compared to kinetically stable pincer ligands, thus provide an alternative pathway for oxide transfer. Indeed, there exist examples of oxide transfer from coordinated CO₂ to chelate or pendant phosphino co-ligands in Ni systems.¹⁷ This strategy, to generate PC_{carbene}P complex **2** from **1**, was demonstrated most successfully using bis(dicyclohexylphosphino)methane (dcpm) and bis(diphenylphosphino)methane (dppm) where oxide transfer to the bisphosphine co-ligand at 100 °C competed with oxide transfer to the pincer ligand phosphino group. After oxide transfer, the reduced binding properties of the partially oxidized bisphosphine ligand enables PMe₃ to displace the chelate ligand and generate complex **2** (Fig. 6).

We further investigated the competitive transfer of the oxide onto dppm or the pincer ligand by synthesizing complex **5**. Complex **5** is an η^2 -carbonyl complex similar to **1**, where the two PMe₃ co-ligands have been replaced by a single dppm ligand (Fig. 8). Notably, the P–Co–P angle of 95.9(1)° in the

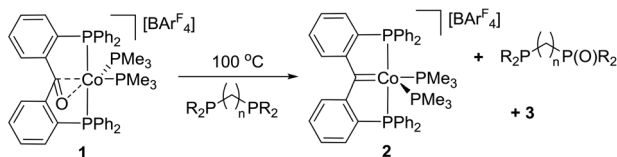


Fig. 6 Oxide transfer to a chelate bisphosphine ligand to generate complex **2**. Yield of **2** and **3**: 30% (**2**), 31% (**3**) (C₂PCH₂PCy₂), 39% (**2**), 36% (**3**) (Ph₂PCH₂PPh₂), 2% (**2**), 22% (**3**) (Ph₂P(CH₂)₂PPh₂), 8% (**2**), 24% (**3**) (Ph₂P(CH₂)₃PPh₂).

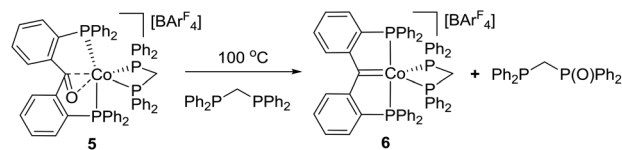


Fig. 7 Heating complex **5** with a dppm co-ligand in the presence of an equivalent of dppm led exclusively to oxide transfer onto the dppm ligand (as opposed to pincer) to provide **6** in 41% yield.

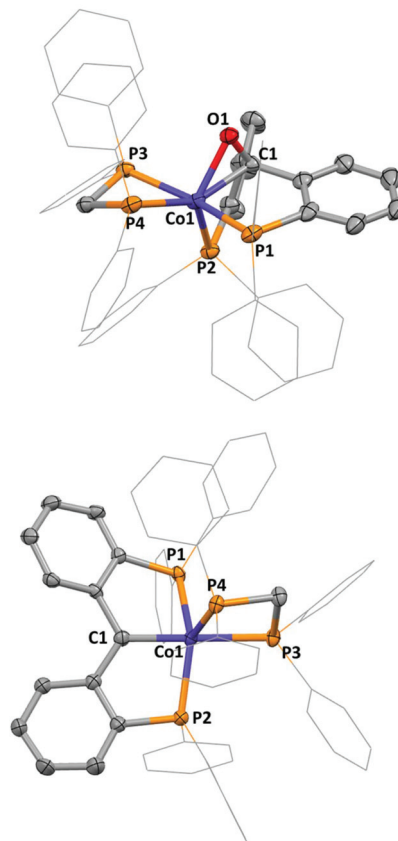


Fig. 8 Molecular structures of **5** (top) and **6** (bottom). Hydrogen atoms and anions omitted, thermal ellipsoids shown at 50%. Selected bond distances (Å) and angles (°), **5**: Co1–P1, 2.203(1); Co1–C1, 2.005(3); C1–O1, 1.311(4); P1–Co1–P2 95.9(1); C1–Co1–P4, 150.4(1), **6**: Co1–P1, 2.231(1); Co1–C1, 1.923(3); Co1–P3, 2.287(1); C1–Co1–P2 143.5(1); C1–Co1–P3, 178.6(1).

pincer ligand of **5** is much more acute as compared to **1** (P–Co–P angle of 147.6(1) in **1**).¹³ Heating **5** in the presence of an extra equivalent of dppm led exclusively to oxide transfer to the dppm ligand (Fig. 7). The extra equivalent of dppm displaces the partially oxidized dppm to generate PC_{carbene}P complex **6** in 41% yield. Thus, dynamic ligand exchange between PMe₃ and the chelate ligands likely gives rise to the mixture of **2** and **3** observed in Fig. 6.

In conclusion, we have reported the observation of a direct C–O double bond cleavage mediated by a cobalt centre, resulting in PC_{carbene}P(O) complex **3**. The C–O bond cleavage was determined *in silico* to proceed *via* metal–ligand cooperativity

requiring the decoordination of a pincer phosphino arm, and terminal oxo pathways were calculated to be energetically unfavourable. The utilization of such metal–ligand cooperativity was extended to chelating bis-phosphine co-ligands, allowing transfer of the oxide to dcpm and dpmm co-ligands to generate PC_{carbene}P pincer complex **2**, after the partially oxidized bisphosphine ligands were displaced by added PMe₃, or PC_{carbene}P complex **6**, when complex **5** with a dpmm co-ligand was isolated and heated with dpmm.

Conflicts of interest

The authors declare no competing financial interest.

Acknowledgements

We thank the National University of Singapore and the Singapore Ministry of Education for financial support (WBS R-143-000-A05-112 and R-143-000-697-114). The authors wish to acknowledge the DJEI/DES/SFI/HEA Irish Centre for High-End Computing (ICHEC) for the provision of computational facilities and support.

References

- (a) O. O. James, B. Chowdhury, M. A. Mesubi and S. Maity, *RSC Adv.*, 2012, **2**, 7347; (b) M. C. Valero and P. Raybaud, *Catal. Lett.*, 2013, **143**, 1; (c) J. Cheng, P. Hu, P. Ellis, S. French, G. Kelly and C. M. Lok, *Top. Catal.*, 2010, **53**, 326; (d) M. Ephritikhine, *Chem. Commun.*, 1998, 2549.
- J. C. Bryan and J. M. Mayer, *J. Am. Chem. Soc.*, 1987, **109**, 7213.
- M. Lutz, M. Haukka, T. A. Pakkanen and L. H. Gade, *Organometallics*, 2001, **20**, 2631.
- S. L. Marquard, M. W. Bezpalko, B. M. Foxman and C. M. Thomas, *J. Am. Chem. Soc.*, 2013, **135**, 6018.
- (a) H. Braunschweig, M. Burzler, K. Radacki and F. Seeler, *Angew. Chem., Int. Ed.*, 2007, **46**, 8071; (b) J. Bauer, H. Braunschweig, A. Damme, J. O. C. Jimenez-Halla, T. Kramer, K. Radacki, R. Shang, E. Siedler and Q. Ye, *J. Am. Chem. Soc.*, 2013, **135**, 8726.
- E. Spaltenstein, R. R. Conry, S. C. Critchlow and J. M. Mayer, *J. Am. Chem. Soc.*, 1989, **111**, 8741–8742.
- E. Poverenov, I. Efremenko, A. I. Frenkel, Y. Ben-David, L. J. W. Shimon, G. Leituss, L. Konstantinovski, J. M. L. Martin and D. Milstein, *Nature*, 2008, **455**, 1093.
- M. K. Goetz, E. A. Hill, A. S. Filatov and J. S. Anderson, *J. Am. Chem. Soc.*, 2018, **140**, 13176.
- (a) M. H. Chisholm and J. A. Klang, *J. Am. Chem. Soc.*, 1989, **111**, 2324; (b) T. P. Blatchford, M. H. Chisholm, K. Folting and J. C. Huffman, *J. Chem. Soc., Chem. Commun.*, 1984, 1295; (c) M. H. Chisholm, C. E. Hammond, V. J. Johnston, W. E. Streib and J. C. Huffman, *J. Am. Chem. Soc.*, 1992, **114**, 7056; (d) B. C. Gates, *Angew. Chem., Int. Ed. Engl.*, 1993, **32**, 228.
- (a) E. K. Van Den Beuken and B. L. Feringa, *Tetrahedron*, 1998, **54**, 12985; (b) J. Park and S. Hong, *Chem. Soc. Rev.*, 2012, **41**, 6931; (c) I. Bratko and M. Gómez, *Dalton Trans.*, 2013, **42**, 10664; (d) A. L. Gavrilova and B. Bosnich, *Chem. Rev.*, 2004, **104**, 349; (e) P. J. Steel, *Acc. Chem. Res.*, 2005, **38**, 243.
- (a) G. van Koten and D. Milstein, *Organometallic Pincer Chemistry*, in *Topics in Organometallic Chemistry*, Springer, Berlin, 2013, vol. 40; (b) G. van Koten and R. A. Gossage, *The Privileged Pincer-Metal Platform: Coordination Chemistry & Applications*, Springer, 2015.
- (a) E. A. LaPierre, M. L. Clapson, W. E. Piers, L. Maron, D. M. Spasyuk and C. Gendy, *Inorg. Chem.*, 2018, **57**, 495; (b) M. J. Ingleson, M. Pink, H. Fan and K. G. Caulton, *J. Am. Chem. Soc.*, 2008, **130**, 4262; (c) L. J. Murphy, A. J. Ruddy, R. McDonald, M. J. Ferguson and L. Turculet, *Eur. J. Inorg. Chem.*, 2018, 4481–4493.
- S. Sung, Q. Wang, T. Krämer and R. D. Young, *Chem. Sci.*, 2018, **9**, 8234.
- (a) D. V. Gutsulyak, W. E. Piers, J. Borau-Garcia and M. Parvez, *J. Am. Chem. Soc.*, 2013, **135**, 11776; (b) L. E. Doyle, W. E. Piers and J. Borau-Garcia, *J. Am. Chem. Soc.*, 2015, **137**, 2187; (c) P. E. Rothstein, C. C. Comanescu and V. M. Iluc, *Chem. – Eur. J.*, 2017, **23**, 16948; (d) C. C. Comanescu and V. M. Iluc, *Chem. Commun.*, 2016, **52**, 9048; (e) C. C. Comanescu and V. M. Iluc, *Polyhedron*, 2018, **143**, 176; (f) S. Sung, T. Joachim, T. Krämer and R. D. Young, *Organometallics*, 2017, **36**, 3117; (g) S. Sung and R. D. Young, *Dalton Trans.*, 2017, **46**, 15407; (h) C. C. Comanescu and V. M. Iluc, *Organometallics*, 2014, **33**, 6059; (i) C. C. Comanescu and V. M. Iluc, *Organometallics*, 2015, **34**, 4684; (j) P. Cui, C. C. Comanescu and V. M. Iluc, *Chem. Commun.*, 2015, **51**, 6206; (k) P. Cui and V. M. Iluc, *Chem. Sci.*, 2015, **6**, 7343; (l) R. J. Burford, W. E. Piers and M. Parvez, *Organometallics*, 2012, **31**, 2949; (m) J. R. Logan, W. E. Piers, J. Borau-Garcia and D. M. Spasyuk, *Organometallics*, 2016, **35**, 1279; (n) L. E. Doyle, W. E. Piers, J. Borau-Garcia, M. J. Sgro and D. M. Spasyuk, *Chem. Sci.*, 2016, **7**, 921; (o) E. A. LaPierre, W. E. Piers and C. Gendy, *Organometallics*, 2018, **37**, 3394; (p) E. A. LaPierre, W. E. Piers and C. Gendy, *Dalton Trans.*, 2018, **47**, 16789; (q) E. A. LaPierre, W. E. Piers, D. M. Spasyuk and D. W. Bi, *Chem. Commun.*, 2016, **52**, 1361; (r) K. S. Feichtner and V. H. Gessner, *Chem. Commun.*, 2018, **54**, 6540.
- (a) J. Cooper and T. Ziegler, *Inorg. Chem.*, 2002, **41**, 6614; (b) K. H. Hopmann, *Organometallics*, 2016, **35**, 3795; (c) M. Besora, P. Vidossich, A. Lledós, G. Ujaque and F. Maseras, *J. Phys. Chem. A*, 2018, **122**, 1392; (d) R. E. Plata and D. A. Singleton, *J. Am. Chem. Soc.*, 2015, **137**, 3811; (e) D. H. Wertz, *J. Am. Chem. Soc.*, 1980, **102**, 5316.
- M. Kazemi and J. Aquvist, *Nat. Commun.*, 2015, **6**, 7293.
- (a) C. Bianchini, C. Mealli, A. Meli and M. Sabat, *Inorg. Chem.*, 1984, **23**, 2731; (b) J. S. Anderson, V. M. Iluc and G. L. Hillhouse, *Inorg. Chem.*, 2010, **49**, 10203.